# Ultra Wideband Indoor Radio Propagation Channel Analysis Using a 3-D Beam Tracing Method - Preliminary Results

***Fabrício J. B. Barros*, *Emanoel Costa, Gláucio L. Siqueira***

Centro de Estudos em Telecomunicações (CETUC), Pontifícia Universidade Católica do Rio de Janeiro (PUC-Rio), Rua Marquês de São Vicente 225, 22451-900 Rio de Janeiro RJ BRASIL, E-mails: fabricio@cetuc.puc-rio.br, epoc@cetuc.puc-rio.br, glaucio@cetuc.puc-rio.br

## Abstract

This paper presents the results from an ultra wideband (UWB) indoor measurement campaign and describes a 3D beam trace pyramidal method that allows one to characterize the channel over a bandwidth of 850 MHz. The UWB channel characteristics are assessed in terms of mean delay, delay spread and coherence bandwidth.

## 1. Introduction

The interest in the use of the ultra wideband (UWB) technique for wireless communication has motivated the development of models to predict the corresponding radio indoor propagation. Recently, several models using ray tracing methods have been proposed for the UWB radio channel [1-3]. However, these models still do not overcome the well-known aliasing problem due the discrete number of rays emitted from the source.

The beam tracing methods eliminate the aliasing problem by dealing with beams that represent an infinite number of rays in a given space region. The beams are recursively traced from a source through the environment. Each originated beam from the source will create successive sequences of transmitted and reflected beams. After tracing beams, rays within each sequence of beams are tracked from the receiver back to the transmitter.

In general, the beam tracing method has been used in a variety of applications: illumination [4], visibility determination [5], and acoustic modeling [6-7]. However, to the best of the authors' knowledge, modeling the UWB channel using beam tracing has not been widely reported in the open literature so far. This paper applies a pyramidal beam trace method to model the UWB channel temporal dispersion in an indoor environment. It also discusses the measurements performed for future comparisons with the results from the proposed method.

## 2. Beam Tracing Model

To better explain the beam tracing model, it will be partitioned into four distinct phases: spatial subdivision, beam emission, path generation and channel characterization.

### 2.1. Spatial Subdivision

In this phase, a spatial subdivision is constructed by partitioning the environment, shown in figure 1(a), into 3D convex polyhedral regions called cells. Before this procedure, the walls with doors and windows are subdivided into convex polygonal faces, represented by the red polygons observed in figure 1 (b). Also note in figures 1(c) and 1(d) that additional cells ("D" and "E") have been created by the partition of the environment. Therefore, each cell is itself convex and bounded by a group of planar convex faces. The corresponding representation is stored into a data structure including: coordinates of faces, faces of each cell, unit vectors of faces and constitutive parameters of cells and faces.

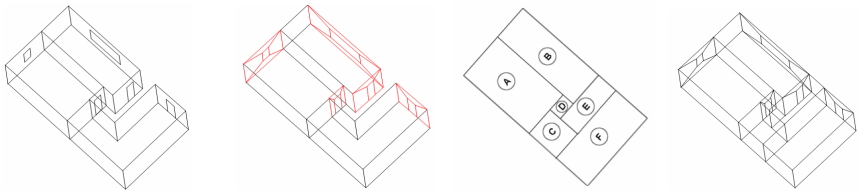


(a) (b) (c) (d)

Figure 1-Spatial subdivision: (a) 3-D environment; (b) 3-D environment with convex polygonal faces; (c) 2-D cell partition; and (d) 3-D cell partition.

## 2.2. Beam Emission

The present beam-tracing method emits pyramidal beams, each represented by a vertex V and a polygonal convex base, as sketched in figure 2. The initial beams are characterized by the transmitter (Tx) and the faces of the cell that contains Tx. In general, the incidence of a beam onto a cell face is processed by determining the intersection between the face and the beam. A transmitted beam (into the neighbor cell) is constructed by the intersection and the original vertex. A reflected beam is generated by the intersection and by mirroring the original vertex with respect to the face, as illustrated in figure 3. Figure 4 partially illustrates the beam tracing emission through a 2D environment. The cell boundaries are given by opaque (solid black line) and transparent (solid red line) faces. The initial beams are traced in the cell containing the source point. Six beams with vertex Tx1 and bases given by the boundary polygons ("s", "t", "i", "h", "g" and "f") of cell "A" are created. For example, transmission of the beam "Tg" through the cell boundary labeled "g" results in a transmitted beam (TgTp). This beam is subdivided when reaches face "p" in another transmitted beam (TgTpTz) in cell "D" and three reflected beams (TgTpRj, TgTpRk and TgTpRl) in cell B. These procedures continue recursively for each beam until a maximum number of transmitted and reflected beams is reached.

The beams are stored in nodes of a beam tree data structure [7]. Each node of the beam tree stores an indication of the polyhedral beam and the face recently traversed by the beam. Thus, for each beam, it is possible to identify the previous and following beams, an essential information used during the path generation phase. Figure 5 presents the beam tree corresponding to the environment transmission shown in figure 4.

## 2.3. Path Generation

For each beam containing the receiver position, a ray is traced from the receiver toward the transmitter, using the beam tree data structure.

The cell containing the receiver is initially identified. Each beam tree node associated with that cell is checked to see whether the beam stored in that node contains the receiver. If it does, a ray from the receiver to the transmitter is generated by interactive intersection with the cell boundaries stored with the predecessor nodes. Figure 6 shows the ray generation for a particular receiver position Rx.

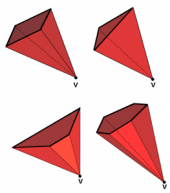

Figure 2- Pyramidal Beams.

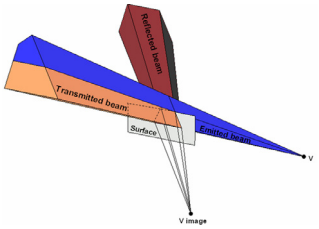


Figure 3- Transmitted and reflected beams.

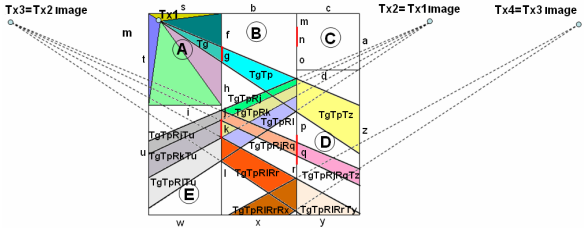


Figure 4-Beam emission.

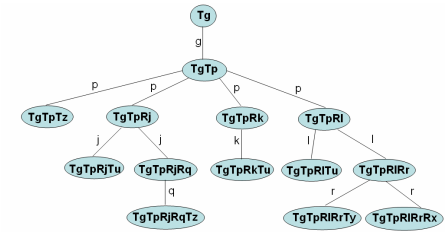


Figure 5-Beam tree.

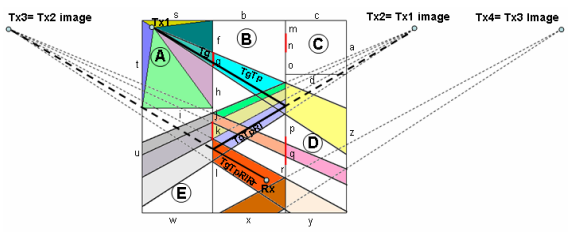


Figure 6-ray generation.

## 2.4. Channel Characterization

After tracing rays, the electromagnetic field for both vertical and horizontal polarizations are calculated using geometric optics (GO) [8] to obtain the channel frequency transfer function, given by:

$$H(f) = \sum_{n=1}^{N} a_n \, e^{-j2\pi f \tau_n}, \tag{1}$$

where N is the number of rays , $a_n$ is the field amplitude of each ray, $\tau_n$ represents the ray delay and $f$ the frequency. It should be observed that the ray parameters are calculated at a large number of frequencies uniformly distributed along

the ultra wide bandwidth of the channel. The impulse response is obtained by applying the inverse Fourier transform to the discrete number of frequency response values resulting from equation (1). Based on the impulse response, parameters such as the power delay profile, the mean delay, the delay spread and the coherence bandwidth are calculated and used to analyze the channel characteristics [9].

## 3. Measurement Procedures and Environment

A Vector Network Analyzer (VNA) HP 8714ET was used to measure the channel impulse response by consecutively exciting 1601 uniformly spaced sinusoidal carriers over a bandwidth of 850 MHz varying from 950 MHz to 1800 MHz. The VNA sweeps the frequency band and reports magnitude and phase data from the radio channel. For the signal transmission and reception, two UWB identical antennas were built [10].

The measurements were conducted in an indoor environment corresponding to the corridors of CETUC, PUC-Rio. In this environment, line-of-sight (LOS) conditions along the corridor A1 and non line-of-sight (NLOS) conditions along the corridors A2 and A3 have been investigated. The measurement layout is detailed in figure 7 (distances are in meters).

In the environment, the receiver (RX) was placed at a fixed position while the transmitter (TX) was moved through the environment around 147 different positions. Consecutive positions are separated by 0.5 meters. The heights of the transmitter and the receiver were fixed at 1.5 meters.

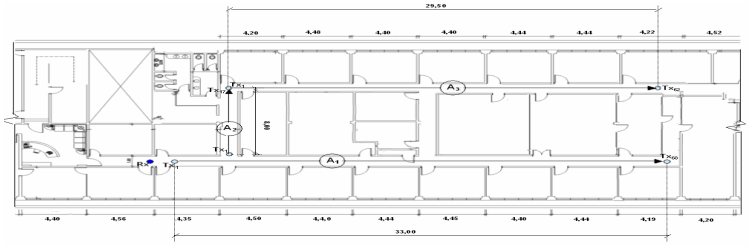

Figure 7- CETUC floor plan and measurement layout.

TABLE I-CHANNEL PARAMETER RESULTS

| Receiver location | Mean Delay [ns] | Delay Spread [ns] | Coherence Bandwidth [MHz] | |
|---|---|---|---|---|
| | | | C=0.7 | C=0.9 |
| Corridor A1 | 93.51 | 47.38 | 12.89 | 3.25 |
| Corridor A2 | 50.99 | 24.29 | 7.74 | 3.77 |
| Corridor A3 | 125.68 | 35.43 | 5.56 | 2.62 |

## 4. Simulated and Measured Results

The measurement results are assessed in terms of mean delays, delay spreads and coherence bandwidths for thresholds of 70 % (C=0.7) and 90% (C=0.9) of the maximum value. Table I above shows the average results.

On both LOS and NLOS measurements, the mean delay and delay spread trends increased with distance while the coherence bandwidth decreases with distance. Figure 8 shows the temporal dispersion parameters as a function of the separation TX-RX along the corridor A1. In this figure, in the first half of the distance between the transmitter and the receiver, an increasing trend was verified in mean delay and delay spread values. However, in the second half of the distance, a trend toward stabilization of mean delay values and a decline in delay spread values was noticed. This trend is due to the transmitter proximity to the wall at the corridor's end, providing a reflected signal that is added to the direct signal, reducing the relative importance of contributions from signals reflected in the lateral walls and decreasing the delay spread values. The coherence bandwidth results presented an inverse trend compared to the mean delay and delay spread values. Additional details on the measured results can be found in Barros et al. [11].

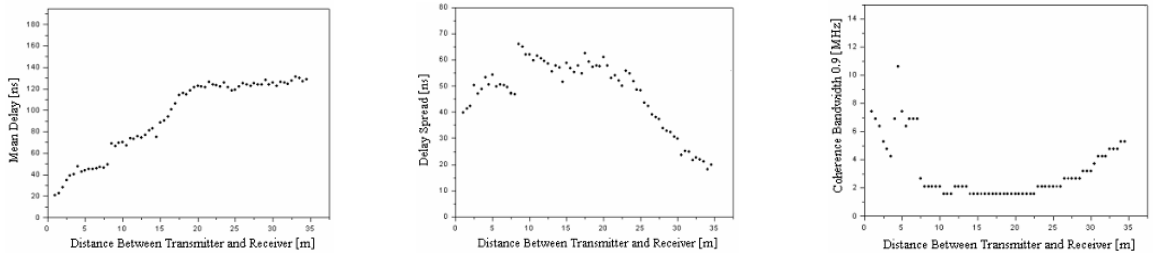


(a) (b) (c)

Figure 8-Temporal dispersion parameters: (a) Mean delay; (b) Delay spread; and (c) Coherence bandwidth with C=0.9.

The results from the beam-tracing model are related to the first two phases: spatial subdivision and beam emission. Figure 9 shows the beam emission inside the CETUC environment. To facilitate visualization, the transmitter has been located inside an office.

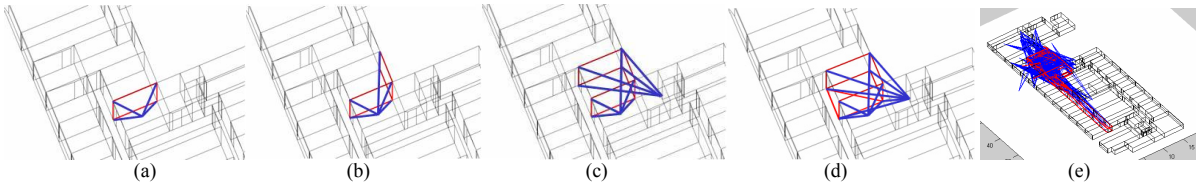

(a) (b) (c) (d) (e)

Figure 9- 3D Beam emission: (a) One beam; (b) Two beams; (c) Three beams; (d) Four beams; and (e) Four hundred beams.

## 5. Conclusion

The results from frequency-domain UWB propagation measurements have shown that the delay spread values increase for LOS and NLOS conditions, while the coherence bandwidth decrease for both conditions. The results reported here are important for other channel modeling purposes.

Preliminary results from a 3D pyramidal beam tracing method to determine reflection and transmission paths through an indoor environment have also been presented. The beam emission is performed only once for a source and the beam tree data structure store all sequence of beams originating at it. This enables a fast and unambiguous generation of all propagation paths between each observation point and the source. From this information, the corresponding channel transfer function and its parameters can be determined.

## 6. Acknowledgments

Fabrício J. B. Barros is supported by a fellowship from CAPES (Coordenação de Aperfeiçoamento de Pessoal de Nível Superior) during the present work.

## 7. References

1. J. Diskin, and C. Brennan, "Accelerated Ray-Tracing for Indoor Ultra-Wideband Propagation Modelling," *Vehicular Technology Conference,* Dublin, 2007, pp. 418-422.

2. G. Tiberi, S. Bertine, W. Q. Malik, A. Monorchio, D. J. Edwards, and G. Manara, "An Efficient Ray Tracing Propagation Simulator for Analyzing Ultrawideband Channels," *IEEE International Conference on Ultra-WideBand,* Singapore, 2007, pp. 794-799.

3. Y. Lostanlen and G. Goungeon, "Introduction of Diffuse Scattering to Enhance Ray-Tracing Methods for the Analysis of Deterministic Indoor UWB Radio Channels (Invited Paper)," *International Conference on Electromagnetics in Advanced Applications,* Torino, 2007, pp. 903-906.

4. P. Heckbert, and P. Hanrahan, "Beam Tracing Polygonal Objects,**"***ACM Computer Graphics,* **18**, July 1984, pp. 119-127.

5. C. B. Jones, "A new approach to the 'hidden line' problem," *The Computer Journal*, Oxford University Press.

6. T. Funkhouser, N. Tsingos, I. Carlbom, G. Elko, M. Sondhi, J. West, G. Pingali, P. Min and, A. Ngan, "Beam Trace Method for Interactive Architectural Acoustics," *J. Acoustical Society of America*, **115**, February 2004, pp. 739-756.

7. T. Funkhouser, I. Carlbom, G. Elko, G. Pingali, M. Sondhi and, J. West "A Beam Tracing Approach to Acoustic Modeling for Interactive Virtual Environments," *Proceedings of the 25th annual conference on Computer graphics and interactive techniques*, July 1998, pp. 21-32.

8. W. S. Lee, "Electromagnetic Reflection from a Conducting Surface-Geometrical Optics Solution". *IEEE Transactions on Antennas and Propagation*, **23**, March 1975, pp. 184-191.

9. J. D. Parson, *Mobile Radio Propagation Channel*, *First edition*, New York, John Wiley & Son, 1992, pp. 184-186.

10. J. R. Bergman, "On the Design of Broad Band Omnidirectional Compact Antennas," *IEEE Microwave and optical Technology Letters*, **39**, October 2003, pp. 418-422.

11. F. J. B. Barros, R. D. Vieira, and G. L. Siqueira, "Measurements and Analyze of UWB Channel Temporal Dispersion," *Thirty-Ninth Asilomar Conference on Signals*, Pacific Grove, CA, 2005, pp. 971-975.